

Technical Note

Central Brightening Due to Constructive Interference With, Without, and Despite Dielectric Resonance

Christopher M. Collins, PhD,* Wanzhan Liu, MS, Weston Schreiber, Qing X. Yang, PhD, and Michael B. Smith, PhD

Purpose: To aid in discussion about the mechanism for central brightening in high field magnetic resonance imaging (MRI), especially regarding the appropriateness of using the term *dielectric resonance* to describe the central brightening seen in images of the human head.

Materials and Methods: We present both numerical calculations and experimental images at 3 T of a 35-cm-diameter spherical phantom of varying salinity both with one surface coil and with two surface coils on opposite sides, and further numerical calculations at frequencies corresponding to dielectric resonances for the sphere.

Results: With two strategically placed surface coils it is possible to create central brightening even when one coil alone excites an image intensity pattern either bright on one side only or bright on both sides with central darkening. This central brightening can be created with strategic coil placement even when the resonant pattern would favor central darkening. Results in a conductive sample show that central brightening can similarly be achieved in weakly conductive dielectric materials where any true resonances would be heavily damped, such as in human tissues.

Conclusion: Constructive interference and wavelength effects are likely bigger contributors to central brightening in MR images of weakly conductive biological samples than is true dielectric resonance.

Key Words: calculations; B_1 ; dielectric resonance; MRI; interference; surface coil

J. Magn. Reson. Imaging 2005;21:192–196.
© 2005 Wiley-Liss, Inc.

STRONG CENTRAL BRIGHTENING has been observed in magnetic resonance imaging (MRI) of the human head using volume coils at high B_0 field strength and

high B_1 field frequency (1–3). Recently there has been some discussion in the literature about the appropriateness of attributing this brightening to dielectric resonance (4–8), as it has been previously (1,2). While it is certain that B_1 wavelengths are on the order of dimensions of the human body at these frequencies, relatively high tissue conductivity inhibits the creation of strong resonances (4–8), and alternative explanations for the observed central brightening are warranted.

A true dielectric resonance is characterized by relatively large oscillating electromagnetic fields in and around an object with a frequency of oscillation near a natural frequency for the object, and elicited by a relatively small stimulus near that natural frequency. The natural resonant frequencies for an object are determined by the geometry and electrical properties of the object, as well as the electrical properties of the surrounding medium. A single object typically has several different resonant modes at several different frequencies, each with a characteristic electromagnetic field pattern (8–11). For some simple shapes, these frequencies and the characteristic field patterns can be calculated with analytical methods (11). But classically, the term *resonance* refers to field intensity as a function of frequency more than as a function of position.

Although other authors have pointed out the lack of strong true resonances in biological tissues, they have not offered an easily understandable alternative explanation for observed central brightening. An enhancement of magnetic field strength near the center of an object can be created by a number of ways, and is not by itself evidence of a dielectric resonance. For example, midway between sources of traveling waves with currents in opposing directions (or 180° out of phase) is a location of constructive magnetic field interference at any frequency, provided the waves from each source travel through the same media for the same distance. This can occur even in an empty coil if the frequency is high enough for the wavelength to be on the order of the coil dimensions. We suggest that it is the combination of multiple current-carrying elements in the coil and wavelength effects in the sample leading to constructive and destructive interference, rather than true dielectric resonance, that causes central brightening in the human head when imaged with a volume coil. Here we show simple cases where central brightening due to

Center for NMR Research, Department of Radiology, Pennsylvania State University College of Medicine, Hershey, Pennsylvania.

Contract grant sponsor: NIH; Contract grant number: R01 EB000454

Continuation of work presented at the 11th Annual Meeting of ISMRM, Toronto, Canada, 2003. p. 2391.

*Address reprint requests to: C.M.C., Center for NMR Research, NMR/MRI Building, Department of Radiology H066, The Pennsylvania State University College of Medicine, 500 University Dr., Hershey, PA 17033. E-mail: cmcollins@psu.edu

Received June 21, 2004; Accepted October 13, 2004.

DOI 10.1002/jmri.20245

Published online in Wiley InterScience (www.interscience.wiley.com).

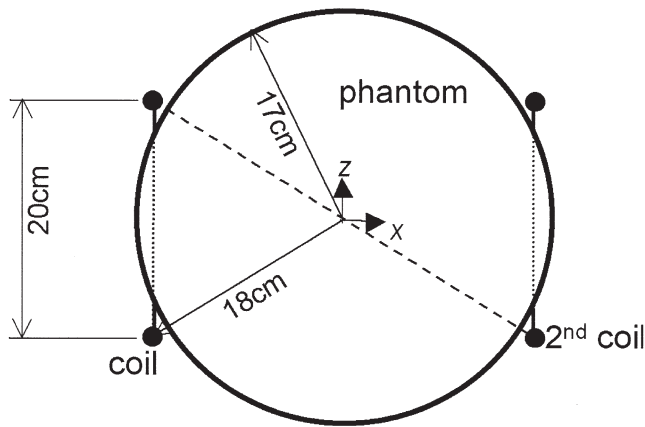


Figure 1. Arrangement of circular surface coil(s) and spherical water phantom. Dashed line is drawn between currents of opposite direction. Midpoint of dashed line, at center of sample, is location of constructive magnetic field interference.

interference by careful placement of the current sources is achieved in different cases, regardless of the field patterns associated with natural resonance of the sample, and even in the absence of any strong resonant field pattern.

MATERIALS AND METHODS

A 35-cm-diameter spherical flask was used in all experiments. To demonstrate dielectric resonances when the flask was filled with water, a 6.0-cm-diameter transmit coil and a 3.0-cm-diameter tracking coil were placed on opposite sides of the flask, and the ratio of the voltage induced in the tracking coil to that used to drive the transmit coil was recorded as a function of frequency when the flask was filled with air (conductivity ≈ 0 S/m, relative permittivity ≈ 1) and with water (conductivity ≈ 0 S/m, relative permittivity ≈ 78) using a Hewlett Packard 4195A Network/Spectrum analyzer.

MR images were acquired with a 3-T Medspec S300 system (Bruker Biospin Corp., Ettlingen, Germany). Two surface coils (20.0 cm diameter) were driven in parallel at 125.44 MHz. Two gradient-echo images (TE = 6.0 msec, TR = 2000 msec, matrix size = 256×256 , field of view (FOV) = 40×40 cm) were acquired on the coronal plane passing through the middle of the sphere, each with a low flip angle, the first with only one coil present and the other with both coils on opposite sides of the flask. This experiment was repeated after adding 30 g of table salt to the flask and mixing well to achieve a salinity of approximately 23.3 mM, resulting in a conductivity of 0.26 S/m—about halfway between the conductivities of brain and fat at 125 MHz.

The experimental MR situations were modeled, as closely as possible, with the finite difference time domain (FDTD) method and methods of analysis published previously (12,13) using a 5.0-mm grid resolution. All FDTD problems were prepared and solved with the aid of commercially available software (xFDTD, Remcom, State College, PA). Similar calculations were repeated at 94 and 138 MHz—frequencies coinciding with natural resonances of the spherical flask. Coil and sample ar-

angement for both calculation and experiment is illustrated in Fig. 1.

RESULTS

The ratio of the voltage induced in the tracking coil to that used to drive the transmit coil as a function of frequency when the flask was filled with air and with water is presented in Fig. 2. Resonances are apparent at frequencies where the voltage induced in the tracking coil is much larger when the flask is filled with water than when it is filled with air. The first and second resonances are centered at about 94 and 138 MHz, respectively.

Experimental images acquired at 125 MHz are shown in Fig. 3, with the corresponding simulated images shown in Fig. 4. Even though this frequency is between resonances (Fig. 2), when only one coil is used to create a field in pure water a signal intensity distribution having bright regions adjacent to and opposite the coil, with central darkening in between, is created. When two strategically placed coils are used, however, the image intensity pattern is one having central brightening.

When only one coil is used to create a field in a 23.3 mM NaCl solution, a signal intensity distribution having only a bright region adjacent to the coil is created, but when two strategically placed coils are used, the image intensity pattern is, again, one having central brightening. The presence or absence of a second coil in simulation had no noticeable effect on the fields when the coil was not driven. No parallel imaging techniques were used in this work. Because the coil currents during reception are induced by precessing nuclei in the sample, the receptivity pattern for each receive coil in an array for parallel imaging should be indicated (by argument of reciprocity) by the pattern when the single coil is driven by itself (but in the presence of other coils to account for coupling). Therefore, images acquired with parallel imaging techniques would be expected to have noticeably different signal intensity patterns than those shown here.

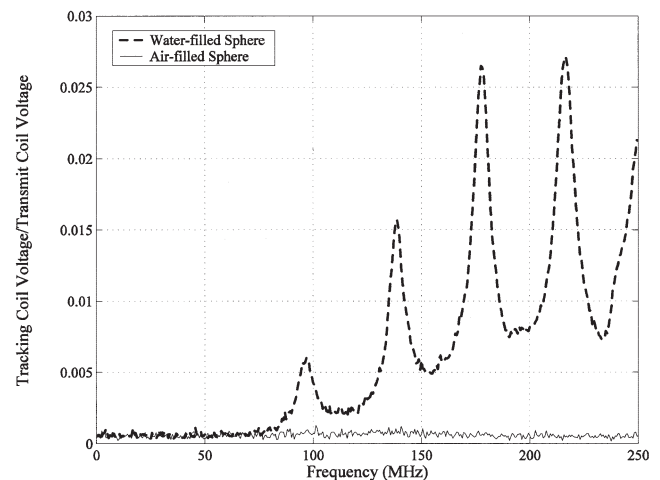


Figure 2. The ratio of the voltage induced in the tracking coil to that used to drive the transmit coil as a function of frequency when the flask was filled with air and with water.

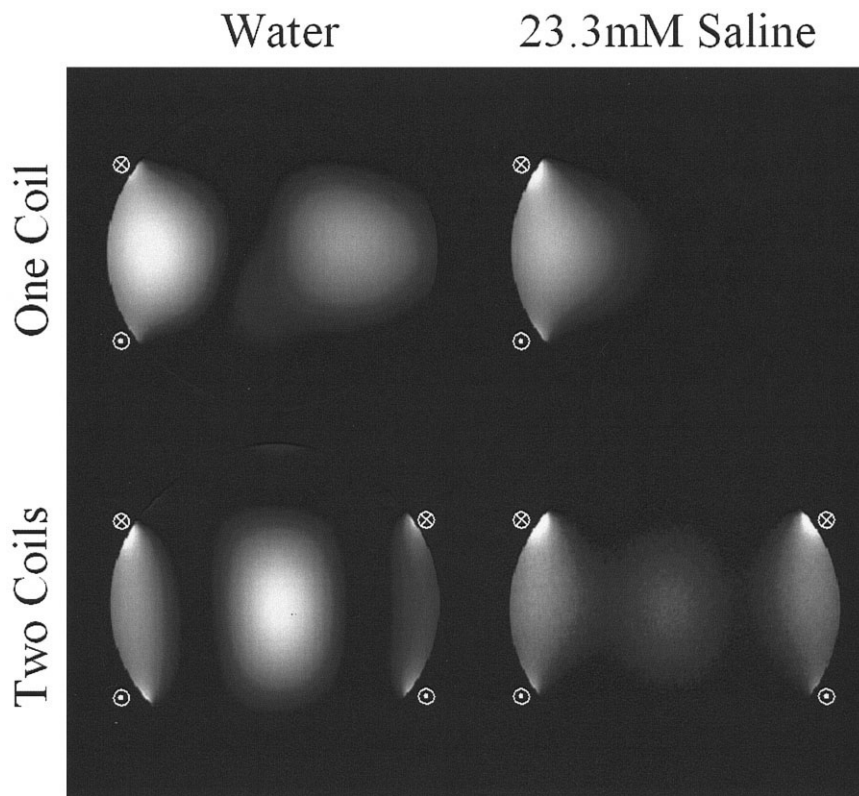


Figure 3. Experimental signal intensity distributions on coronal plane (B_0 oriented in z-direction as in Fig. 1) for sphere of water (left) and 23.3 mM saline (right) excited with one (top of figure) and two (bottom of figure) circular surface coils. When sphere is excited with two coils on opposite sides of the sample, wavelength effects result in constructive interference and bright spot at center of the sample.

The excellent agreement between the experimental images in Fig. 3 and the simulated images in Fig. 4 demonstrates the accuracy of our simulation techniques. Some slight asymmetry in the experimental sin-

gle-coil image acquired in pure water may be due to some slight asymmetry in the flask, such as the presence of a neck, or slight asymmetry in coil current or placement. Further simulations at 94 and 138 MHz

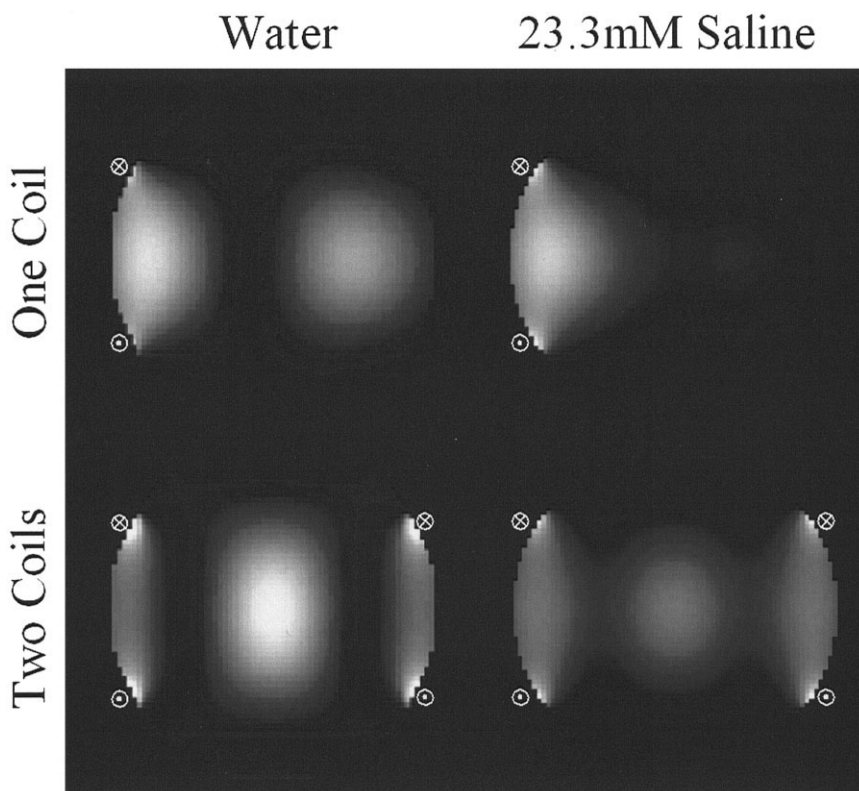


Figure 4. Calculated signal intensity distributions on coronal plane for sphere of water (left) and 23.3 mM saline (right) excited with one (top of figure) and two (bottom of figure) circular surface coils. Results demonstrate excellent agreement with experiment (Fig. 3).

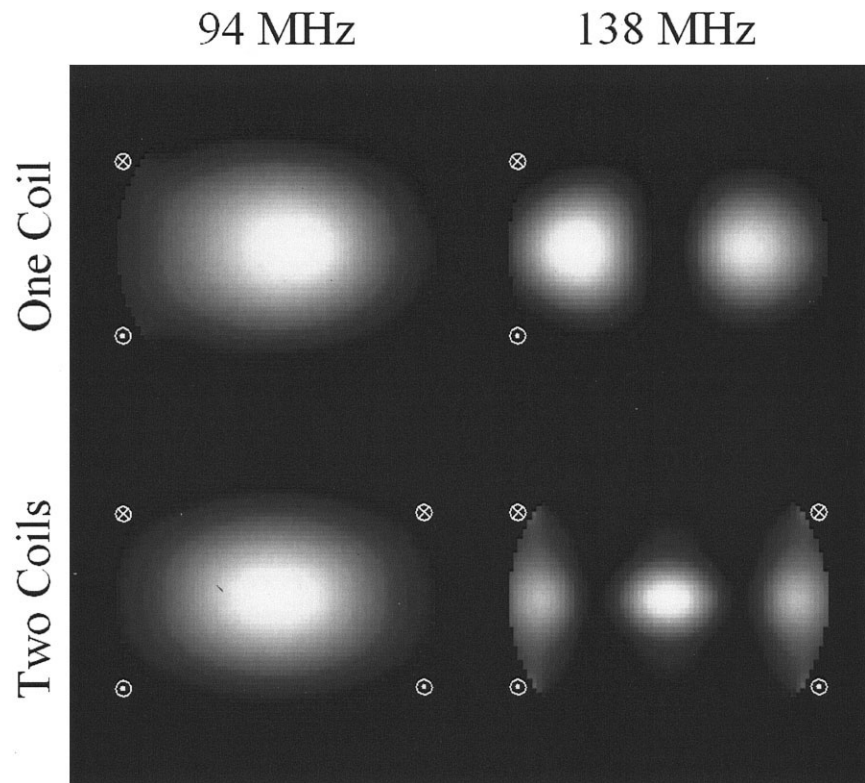


Figure 5. Calculated signal intensity distributions on coronal plane for sphere of water excited with one (top of figure) and two (bottom of figure) circular surface coils at 94 MHz (left) and 138 MHz (right), at frequencies coinciding with the first two dielectric resonances (Fig. 2).

show that central brightening exists when using two strategically placed coils at frequencies coinciding with natural resonances of the sample, even when the field pattern associated with the natural resonance clearly favors central darkening, as at 138 MHz. This result runs counter to logic which suggests that on resonance, the same magnetic field pattern will exist regardless of the excitation method (4).

DISCUSSION

At 94, 125, and 138 MHz the electromagnetic wavelength in water is about 36, 27, and 24 cm, respectively. Thus, at these frequencies it can be useful, conceptually, to think of the B_1 field as being associated with electromagnetic waves originating at the coil elements and interfering within the sample.

In the results presented here, central brightening is seen due to a true dielectric resonance at 94 MHz when one or two coils are used (Fig. 5), but also due to constructive interference between fields from two coils at a frequency off-resonance (125 MHz) at two different sample conductivities (Figs. 3 and 4), as well as to constructive interference between fields from two coils at a resonance at 138 MHz having a field pattern that has a central magnetic field minimum (Fig. 5).

At 94 MHz in pure water, the signal intensity pattern created by one coil yields a signal intensity distribution that is already bright at the center, and the addition of the second coil does not effectively change this pattern except to make it slightly more symmetric.

At either 125 or 138 MHz, when only one coil is used to create a field, the magnetic field pattern results in bright regions adjacent to and opposite the coil, with

central darkening in between. The magnetic field created by a second driven coil on the opposite side significantly alters the field created by the first, and also results in central brightening. This central brightening can be explained by considering a straight line between currents of opposite directions (e.g., dashed line in Fig. 1). In a symmetric system, such as this one, the midpoint of this line will be a location of constructive magnetic field interference at any wavelength, resulting in central brightening in the cases shown here.

Even when the conductivity of the phantom is increased at an off-resonance frequency to further dampen any effects of resonance, constructive interference at the center of the sample can result in central brightening in the presence of two coils at 125 MHz, though only one bright region, adjacent to the coil, is seen in images acquired with one coil. Further increasing the sample conductivity could dampen the penetration of all the fields so much that the fields would be much weaker at the coil center than near the current-carrying elements, even with the effects of constructive interference there (14).

Here we have discussed interference only as from different current sources and have not made mention of interference between primary fields and fields reflected at the boundaries of the object. In fact, interference between the primary and internally reflected fields is very important in determining the field pattern associated with true dielectric resonances, as resonances typically occur when the primary and reflected fields interfere to make a standing wave pattern with a high standing wave ratio. In a conductive medium, such as the human brain or the saline phantom used here, however, all of the fields are attenuated as they propa-

gate, so the reflected waves are of little importance (8) and true dielectric resonances are severely damped, if they can be found at all.

In a quadrature volume coil there are typically as many as 16 conducting elements, each, in theory, directly across the coil from an element carrying current of approximately equal magnitude and opposite phase to its own. Such a situation is ideal for the creation of a region of constructive interference at the center of the coil and, at higher frequencies, bands of destructive interference around it (12,15). This interference pattern can be described as setting up a system of wavelength effects, standing waves, standing wave envelopes, or radio frequency (RF) coil/sample interactions (4,8,14–17), and can result in central brightening without the existence of a true dielectric resonance.

REFERENCES

1. Bomsdorf H, Helzel T, Hunz D, Roschmann P, Tschendel O, Weiland J. Spectroscopy and imaging with a 4 tesla whole-body system. *NMR Biomed* 1988;1:151–158.
2. Barfuss H, Fischer H, Hentschel D, et al. In vivo magnetic resonance imaging and spectroscopy of humans with a 4T whole-body magnet. *NMR Biomed* 1990;3:31–45.
3. Vaughan JT, Garwood M, Collins CM, et al. 7T vs. 4T: RF power, homogeneity, and signal-to-noise comparison in head images. *Magn Reson Med* 2001;46:24–30.
4. Ibrahim T, Lee R, Abduljalil AM, Baertlein BA, Robitaille PM-L. Dielectric resonances and B1 field inhomogeneity in UHFMRI: computational analysis and experimental findings. *Magn Reson Imaging* 2001;19:219–226.
5. Roschmann P. Role of B1 eigenfields of dielectric objects in high-field MRI. In: Proceedings of the 8th Annual Meeting of ISMRM, Denver, 2000. p 151.
6. Kangarlu A, Baertlein BA, Lee R, et al. Dielectric resonance phenomena in ultra high field MRI. *J Comput Assist Tomogr* 1999;23:821–831.
7. Tropp J. Image brightening in samples of high dielectric constant. *J Magn Reson* 2004;167:12–24.
8. Yang QX, Wang JH, Collins CM, et al. Analysis of wave behavior in dielectric sample at high field. *Magn Reson Med* 2002;47:982–989.
9. Strilka RJ, Li S, Martin JT, Collins CM, Smith MB. A numerical study of radiofrequency deposition in a spherical phantom using surface coils. *Magn Reson Imaging* 1998;16:787–798.
10. Wen H, Jaffer FA, Denison TJ, Dueueil S, Chesnick AS, Balaban RS. The evaluation of dielectric resonators containing H₂O or D₂O as RF coils for high-field MR imaging and spectroscopy. *J Magn Reson* 1996;110B:117–123.
11. Gastine M, Courtois L, Dormann JL. Electromagnetic resonances of free dielectric spheres. *IEEE Trans Microwave Theory Tech* 1997;15:694–700.
12. Collins CM, Smith MB. Signal-to-noise ratio and absorbed power as functions of main magnetic field strength and definition of “90°” RF pulse for the head in the birdcage coil. *Magn Reson Med* 2001;45:684–691.
13. Collins CM, Yang QX, Wang JH, et al. Different excitation and reception distributions with a single-loop transmit-receive surface coil near a head-sized spherical phantom at 300 MHz. *Magn Reson Med* 2002;47:1026–1028.
14. Alecci M, Collins CM, Smith MB, Jezzard P. Radio frequency magnetic field mapping of a 3 Tesla birdcage coil: experimental and theoretical dependence on sample properties. *Magn Reson Med* 2001;46:379–385.
15. Ocali O, Atalar E. Ultimate intrinsic signal-to-noise ratio in MRI. *Magn Reson Med* 1998;39:462–473.
16. Tofts PS. Standing waves in uniform water phantoms. *J Magn Reson* 1994;104B:143–147.
17. Sled JG, Pike GB. Standing-wave and RF penetration artifacts caused by elliptic geometry: an electrodynamic analysis of MRI. *IEEE Trans Med Imaging* 1998;17:653–662.